Inorganic Chemistry
Cite This: Inorg. Chem. 2019, 58, 7243−7254
Article
pubs.acs.org/IC

# Novel Heterometallic Uranyl-Transition Metal Materials: Structure, Topology, and Solid State Photoluminescence Properties

Germán E. Gomez,[†] J. August Ridenour,[‡] Nicole M. Byrne,[‡] Alexander P. Shevchenko,[§] and Christopher L. Cahill*[,‡]

[†]Instituto de Investigaciones en Tecnología Química (INTEQUI), Area de Química General e Inorgánica "Dr. G. F. Puelles," Facultad de Química, Bioquímica y Farmacia, Chacabuco y Pedernera, Universidad Nacional de San Luis, Almirante Brown, 1455, 5700 San Luis, Argentina

[‡]Department of Chemistry, The George Washington University, Science and Engineering Hall, 800 22nd Street, NW, Washington, DC 20052, United States

[§]Samara Center for Theoretical Materials Science, Samara University, 34, Moskovskoye shosse, Samara, 443086, Russia

Supporting Information

**ABSTRACT:** Six new uranyl hybrid materials have been synthesized solvothermally utilizing the ligands 2,2′-bipyridine-3,3′-dicarboxylic acid ($\mathbf{H_2L}$) and 2,2′:6′,2′′-terpyridine (**TPY**). The six compounds are classified as either molecular complexes ($I^0O^0$ connectivity), $[(UO_2)(\mathbf{L})(\mathbf{TPY})]\cdot H_2O$ (**1**), $[Ni(\mathbf{TPY})_2][(UO_2)(\mathbf{L})_2]\cdot 3H_2O$ (**2**), and $[Cu(\mathbf{TPY})_2][(UO_2)(\mathbf{L})_2]\cdot 3H_2O$ (**3**), or 3D metal−organic frameworks (MOFs, $I^0O^3$ connectivity), $[Cu_2(UO_2)_2(OH)(C_2H_3O_2)(\mathbf{L})_3(\mathbf{TPY})_2]\cdot 6H_2O$ (**4**), $[Zn_2(UO_2)_2(OH)(NO_3)(C_2H_3O_2)(\mathbf{L})_3(\mathbf{TPY})_2]\cdot 4H_2O$ (**5**), and $Na[Ni(UO_2)_3(OH)(O)(\mathbf{L})_3]\cdot 9H_2O$ (**6**). A discussion of the influence of transition metal incorporation, chelating effects of the ligand, and synthesis conditions on the formation of uranyl materials is presented. The structure of compound **6** is of particular note due to large channel-like voids with a diameter of approximately 19.6 Å. A topological analysis of **6** reveals a new topology with a 9-nodal 3,3,3,3,3,3,3,4,5-connected network, designated **geg1** hereafter. Further, solid state photoluminescence experiments show emission and lifetimes values consistent with related uranyl compounds.

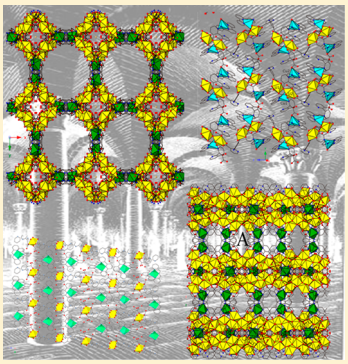

## 1. INTRODUCTION

Research into inorganic−organic hybrid materials in the form of coordination polymers (CPs) or metal organic frameworks (MOFs) has been the focus of significant efforts in materials synthesis owing to their unique properties such as gas sorption,[1] optical luminescence,[2] and heterogeneous catalysis.[3] During the past several years, the synthetic exploration of uranyl ($[UO_2]^{2+}$)-based CPs has garnered more attention owing to the potential for generating a variety of new structural motifs and topological architectures.[4,5] Additionally, uranyl-containing compounds provide a substantive platform for the study of luminescent materials toward potential applications in photocatalysis.[6]

From a structural perspective, the linear geometry of the $[UO_2]^{2+}$ ion and the terminal nature of its "yl" oxygen atoms promote an equatorial arrangement of ligand coordination, explaining the prevalence for quasi-planar 2D polymeric frameworks in many uranyl compounds. One strategy to overcome this 2D structural preference is the use of polytopic linkers to produce out-of plane connectivity, thus assisting in the formation of nanocages, rings, and nanotubes.[7] The incorporation of secondary metal centers, such as d-block transition metals,[8] lanthanides,[9] or other main-group elements,[10] is another synthetic strategy utilized to increase dimensionality in uranyl CPs. In general, the construction of these materials involves the incorporation of two or more metal centers into one compound through multi-topic organic ligands which can selectively coordinate to different metal centers. According to HSAB (hard/soft acid/base) theory, the uranyl cation behaves as a hard acid and has a strong affinity toward O-donor groups (such as carboxylate groups), whereas some transition metal ions are "softer" and may preferentially coordinate to N-donor groups (e.g., pyridine rings). Based on this strategy, the use of a ligand containing both carboxylate and pyridine groups could be promising for designing actinides-transition metals CPs. To that end, we have chosen 2,2′-bipyridine-3,3′-dicarboxylic acid ($\mathbf{H_2L}$) as the multitopic ligand due the presence of both nitrogen and oxygen donor atom moieties, working as a bridge to connect two different metal centers together (Scheme 1).[11] The versatile coordination modes exhibited by a ligand such as $\mathbf{H_2L}$ would give rise to a diverse collection of coordination modes and structural motifs as evidenced by multiple examples in the literature.[12] Moreover, we have included 2,2′:6′2′′ terpyridine (TPY) as an additional ligand, as such "dual ligand" (mostly aromatic amines molecule) strategies have been successful in our

Received: January 30, 2019
Published: April 18, 2019






DOI: 10.1021/acs.inorgchem.9b00255
Inorg. Chem. 2019, 58, 7243−7254

**Scheme 1. Organic Ligands Used in This Study**

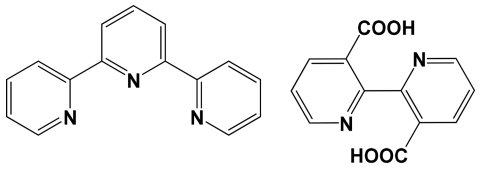


previous efforts to influence uranyl coordination geometry[13] and in others as well.[14]

Herein, three molecular uranyl materials, one homometallic uranyl and two heterometallic uranyl complexes with the $\mathbf{H_2L}$ and **TPY** ligands, $[(UO_2)(\mathbf{L})(\mathbf{TPY})]\cdot H_2O$ (**1**), $[Ni(\mathbf{TPY})_2][(UO_2)(\mathbf{L})_2]\cdot 3H_2O$ (**2**), and $[Cu(\mathbf{TPY})_2][(UO_2)(\mathbf{L})_2]\cdot 3H_2O$ (**3**), along with three 3D heterometallic-uranyl-MOFs, $[Cu_2(UO_2)_2(OH)(C_2H_3O_2)(\mathbf{L})_3(\mathbf{TPY})_2]\cdot 6H_2O$ (**4**), $[Zn_2(UO_2)_2(OH)(NO_3)(C_2H_3O_2)(\mathbf{L})_3(\mathbf{TPY})_2]\cdot 4H_2O$ (**5**), $Na[Ni(UO_2)_3(OH)(O)(\mathbf{L})_3]\cdot 9H_2O$ (**6**), have been synthesized via solvothermal methods. All six compounds (**1**–**6**) were structurally characterized with single-crystal and powder X-ray diffraction techniques and discussed in the context of structurally relevant compounds in the recent literature. Most of the compounds exhibited characteristic uranyl emission, and **6** featured relatively high thermal stability. Further, a topological simplification was performed on compound **6** and revealed a novel 9-nodal 3,3,3,3,3,3,3,4, 5-connected network, hereafter designated **geg1**.

## 2. EXPERIMENTAL SECTION

**2.1. Synthesis.** ***Caution!*** *Although the uranyl acetate dihydrate* $(UO_2(CH_3\text{-}COO)_2\cdot 2H_2O)$ *used in these studies contains depleted uranium, standard precautions for handling radioactive and toxic substances should be followed.* All materials, including 2,2′-bipyridine-3,3′-dicarboxylic acid ($\mathbf{H_2L}$), 2,2′:6′,2″-terpyridine (**TPY**) (Scheme 1), $Ni(CH_3\text{-}COO)_2\cdot 4H_2O$, $Cu(CH_3\text{-}COO)_2\cdot H_2O$, $Zn(NO_3)_2\cdot 6H_2O$, and 2-propanol, were purchased and used without further purification.

All compounds were synthesized via solvothermal methods in 23 mL Teflon-lined Parr autoclaves at varied temperatures, reaction times, amounts of water and 2-propanol, and reactant molar ratios. The pH value of all reactions was adjusted to approximately 5 with two drops of 5 M NaOH. A tabulated summary of synthetic conditions is provided in the Supporting Information (SI) (Table S1). After heating, reaction vessels were removed from the oven and allowed to cool to room temperature over 3 h (**1**–**4**) or rapidly using a water bath (**5**, **6**). Bulk reaction products were washed twice in a sonication bath for 1 h in a 1:1 mixture of water and 2-propanol and air-dried at room temperature. Single crystals (Figure S1) of all compounds (**1**–**6**) suitable for X-ray diffraction were manually isolated. Initial syntheses of compound **6** included the use of **TPY**, which generated mixtures of compounds **2** and **6**. As the structure of **6** does not contain **TPY**, subsequent syntheses were done without the N-donor to generate adequate amounts of compound **6**, without the co-formation of **2**, for spectroscopic studies.

**2.2. Single-Crystal X-ray Structure Determination.** Single crystals from each bulk sample were isolated and mounted on MiTeGen micromounts. Structure determination for each of the single crystals was achieved by collecting reflections using 0.5° $\omega$ scans on a Bruker SMART diffractometer furnished with an APEX II CCD detector using Mo K$\alpha$ ($\lambda$ = 0.71073 Å) radiation at 100 K. The data were integrated using the SAINT software package[15] contained within the APEX III software suite,[16] and an absorption correction was performed using SADABS.[17] The structures of all compounds were solved using intrinsic phasing employing SHELXT-2014.[18] All six compounds were refined using SHELXL-2018[16] contained within the WinGX[19] software suite. In each structure, all non-hydrogen atoms were located via difference Fourier maps and refined anisotropically. Aromatic hydrogen atoms were placed at their idealized positions and allowed to ride on the coordinates of their parent carbon atom ($(U_{iso})$ fixed at $1.2U_{eq}$). Hydrogen atoms on lattice water molecules were found in the Fourier map for OW1 in **1**, OW1 and OW2 in **2**, and OW2 in **3** but were not found for other lattice water molecules in these compounds or in compounds **4**–**6**

**Table 1. Crystallographic Data and Refinement Parameters for Compounds 1–6**

| | 1 | 2 | 3 | 4 | 5 | 6 |
|---|---|---|---|---|---|---|
| empirical formula | $UC_{27}H_{19}N_5O_7$ | $NiUC_{54}H_{38}N_{10}O_{13}$ | $CuUC_{54}H_{36}N_{10}O_{13}$ | $Cu_2U_2C_{68}H_{43}N_{12}O_{24}$ | $Zn_2U_2C_{68}H_{43}N_{12}O_{24}$ | $NaNi_2U_6C_{72}H_{36}N_{12}O_{59}$ |
| FW (g·mol$^{-1}$) | 767.21 | 1331.68 | 1334.51 | 2031.31 | 2018.99 | 3581.72 |
| temp (K) | 100 | 100 | 100 | 100 | 100 | 100 |
| $\lambda$ (Å) | 0.71073 | 0.71073 | 0.71073 | 0.71073 | 0.71073 | 0.71073 |
| crystal system | triclinic | triclinic | triclinic | monoclinic | monoclinic | tetragonal |
| space group | $P\bar{1}$ | $P\bar{1}$ | $P\bar{1}$ | $Cc$ | $Cc$ | $I4_1/acd$ |
| unit cell | | | | | | |
| $a$ (Å) | 8.9630(3) | 9.7784(3) | 9.8119(19) | 26.077(3) | 26.095(4) | 38.156(2) |
| $b$ (Å) | 11.4363(3) | 12.8937(4) | 12.900(3) | 14.2178(12) | 14.149(2) | 38.156(2) |
| $c$ (Å) | 13.5590(4) | 21.3925(6) | 21.450(4) | 21.0657(17) | 21.295(3) | 39.627(2) |
| $\alpha$ (deg) | 106.368(1) | 96.773(2) | 96.512(2) | 90 | 90 | 90 |
| $\beta$ (deg) | 104.783(1) | 91.785(2) | 91.414(2) | 113.187(2) | 113.587(2) | 90 |
| $\gamma$ (deg) | 92.934(1) | 107.031(1) | 106.751(2) | 90 | 90 | 90 |
| volume (Å$^3$) | 1277.98(7) | 2554.75(13) | 2578.3(9) | 7179.4(12) | 7205.6(18) | 57692(7) |
| $Z$ | 2 | 2 | 2 | 4 | 4 | 2 |
| $\rho$ calcd (mg·m$^{-3}$) | 1.994 | 1.731 | 1.719 | 1.879 | 1.861 | 1.664 |
| abs coeff (mm$^{-1}$) | 6.409 | 3.612 | 3.626 | 5.171 | 5.226 | 7.048 |
| $F(000)$ | 732 | 1312 | 1310 | 3908 | 3884 | 26544 |
| $\theta$ range (deg) | 1.631–32.644 | 0.961–31.782 | 0.957–27.161 | 1.665–25.776 | 1.672–26.402 | 4.632–52.324 |
| reflns collected | 58239 | 125387 | 60851 | 44415 | 46391 | 95844 |
| Gof on $F^2$ | 1.058 | 1.041 | 1.021 | 1.054 | 1.016 | 1.061 |
| $R_{int}$ | 0.0230 | 0.0261 | 0.0401 | 0.0434 | 0.0542 | 0.0527 |
| $R1$ [$I > 2\sigma(I)$] | 0.0189 | 0.0183 | 0.0262 | 0.0315 | 0.0388 | 0.0511 |
| $wR2$ [$I > 2\sigma(I)$] | 0.0423 | 0.0458 | 0.0613 | 0.0805 | 0.0897 | 0.1690 |



DOI: 10.1021/acs.inorgchem.9b00255
Inorg. Chem. 2019, 58, 7243–7254

and so were not modeled. A DFIX command was used to fix hydrogen atoms to OW1 in **1**. PART commands were used to model two part atomic disorder in lattice water molecules in compounds **1**, **4**, and **5** (OW1A/B). TWIN/BASF commands were utilized in compounds **4** and **5** as determined by TwinRotMat in Platon[20] (TWIN -100 010 00-1, BASF for **4**: 0.38280, BASF for **5**: 0.24860). The OMIT 0 2 0 command was utilized in compounds **5** and **6** to eliminate reflections affected by the beam stop. ISOR commands were used on atoms C6, C7, and C44 in **4**, N2, C8, C9, C14, and C17 in **5**, and on C25, C26, C32 in **6**. Squeeze was attempted to remove disordered solvent in the large voids present in compound **6**, but was rejected because the void volume is such a large percentage of the overall volume of the compound (~35%) and the removal of that residual electron density did not significantly improve refinement statistics. Figures were prepared with the CrystalMaker[21] program. Data collection and refinement details for compounds **1**–**6** are included in Table 1. Thermal ellipsoid plots are provided in section III in the SI.

**2.3. Powder X-ray Diffraction (PXRD).** Powder X-ray diffraction (PXRD) data on the samples of compounds **1**–**6** (section IV, Figures S8–S13, in the SI) were analyzed and compared with the corresponding simulated patterns. All data were collected on a Rigaku Miniflex (Cu K$\alpha$, $2\theta$ = 3–40°) and were analyzed using the Match! software program.[22]

**2.4. Thermal Analysis.** Thermogravimetric analysis (TGA) was performed on compound **6** with a Shimadzu TGA apparatus under a nitrogen flow of 50 mL min$^{-1}$. The sample was heated from 30 to 800 °C at a heating rate of 5 °C min$^{-1}$ (Figure S14).

**2.5. Solid State Luminescence Measurements.** Data were collected on single crystals of **1**–**6** using a Horiba Jobin Yvon spectrophotometer and processed using Horiba FluorEssence software. The crystals were placed in a quartz NMR tube, which was capped and submerged in a quartz Dewar filled with liquid nitrogen. An excitation wavelength of 365 nm was used, with excitation and emission slits set at 1.5 and 0.5 nm, respectively. Lifetime profiles for all six compounds were obtained using the JobinYvon FluoroHub single photon counting module, and the data were fit using DAS6 software.

## 3. RESULTS AND DISCUSSION

**3.1. Crystal Structures 1–6.** Compound **1** crystallizes in the triclinic space group $P\bar{1}$, and has an asymmetric unit that contains one unique $[UO_2]^{2+}$ center that adopts a pentagonal bipyramidal geometry when coordinated by an **L** ligand and a chelating **TPY** (Figure 1). The U1–O bond distances of the bidentate **L** ligand are 2.2984(1) and 2.2806(1) Å (O3 and O5, respectively), and the **TPY** is bound at U–N distances of 2.5704(1), 2.5855(1), and 2.5812(1) Å (N1, N2, and N3, respectively). The uranyl monomers of **1** are assembled into a supramolecular dimer via hydrogen bonds between a carboxylate, a lattice water molecule, and a nitrogen in a bipyridine ring with heteroatom interactions distances of 2.9450(1) Å (O6–OW1) and 3.0055(1) Å (OW1–N5) (Figure 2). Moreover, the **L** coordination mode can be identified herein as a "malonate mode"[23] owing to its frequent observation in malonate and in some aliphatic dicarboxylates-containing compounds; herein, we refer to this coordination mode as **L-1** as delineated in Figure 3 (along with others observed in compounds **1**–**6**). Further, significant ring torsion is observed in **L** with a torsion angle of 104.6°. The connectivity displayed by the organic and inorganic subunits in **1** allows this compound to be classified as $I^0O^0$, as defined by Cheetham et al.[24] Using this scheme, $I^0$ and $O^0$ denote a connectivity of 0D for both inorganic and organic linkers, and by adding the exponents, the overall dimensionality realized is a 0D molecular complex for **1**.

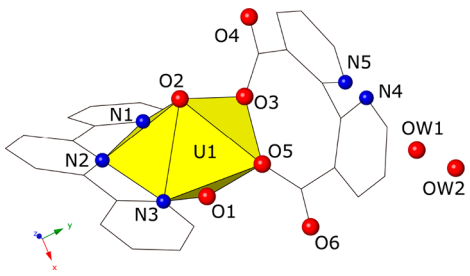


**Figure 1.** Polyhedral representation of compound **1**. Yellow polyhedra represent uranium atoms, red spheres represent oxygen atoms, and blue spheres are nitrogen atoms. All hydrogen atoms were omitted for clarity here and throughout the remainder of the paper.

Compounds **2** and **3** are isomorphous with the only difference being the transition metal (**2** contains Ni and **3** contains Cu), and as such, only compound **2** will be discussed in detail. Compound **2** crystallizes in the triclinic space group $P\bar{1}$. The asymmetric unit is composed of a cationic species, bis(2,2′:6′,2′′-terpyridine)nickel(II) ($[Ni(\mathbf{TPY})_2]^{2+}$), which is charge balanced by an anionic complex, bis(2,2′-bipyridine-3,3′-dicarboxylate)uranyl ($[UO_2(C_{12}H_6N_2O_4)_2]^{-2}$), and three unique lattice water molecules (Figure 4). The asymmetric unit contains two unique uranyl metal centers, both on inversion centers, each coordinated to a single unique **L** ligand (**L-1**, Figure 3) in a bidentate fashion. The U–O distances are 2.3044(1) Å for U1–O2 and O2*, 2.2759(1) Å for U1–O4 and O4*, 2.2717(1) Å for U2–O7, and 2.2910(1) Å for U2–O9. The nickel(II) site, coordinated by two **TPY** molecules with Ni–N bond distances in the range of 1.995(2)–2.916(3) Å, displays a distorted octahedral coordination geometry. Both compounds **2** and **3** can be classified as $I^0O^0$, and such "discrete" f-/d-metal sites as separated by ligand preferences have been reported.[11a,b]

Compounds **4** (Cu) and **5** (Zn) are isomorphous as well, again the only difference being the identity of the transition metal, so only compound **4** will be discussed in detail. Compound **4** crystallizes in the *Cc* monoclinic space group and has an asymmetric unit consisting of a uranyl dimer bridged by an acetate and a hydroxide ligand, two **TPY** chelated $Cu^{2+}$ metal centers, and three unique **L** (**L-2** and **L-3**) ligands, each exhibiting different coordination modes (Figure 5). U1 is coordinated by two of the **L** ligands. The first is in a bidentate fashion (see **L-2** conformation in Figure 3) through U1–O10 and U1–O11 distances of 2.496(7) and 2.462(8) Å, respectively, and the second is monodentate (**L-3**) though a U1–O17 bond distance of 2.338(10) Å. U1 is bridged to U2 through the hydroxide by U1–O3 and U2–O3 distances of 2.312(8) and 2.313(8) Å, respectively, and through a bridging bidentate acetate ligand with bond distances of 2.322(9) Å (U1–O4) and 2.399(10) Å (U2–O5). U2 is further coordinated by two **L** ligands, in the **L-2** bidentate mode through bonds distances of 2.458(8) Å (O8) and 2.491(6) Å (O9) and in the **L-3** monodentate mode through a bond distance of 2.307(8) Å (O12). Assembling only uranyl dimers together with **L-2** ligands forms 1D chains in approximately the [0 0 1] direction (Figure 6). Both uranyl centers exhibit pentagonal bipyramidal coordination geometries. The two crystallographically independent $Cu^{2+}$ centers are both chelated by the tridentate **TPY** ligands through bond distances that range from 1.946(10) to 2.031(9) Å and bound together through **L-3** ligands that assemble only copper units into a 1D chain in the [0 1 0] direction (Figure 6). Offset $\pi$-stacking


DOI: 10.1021/acs.inorgchem.9b00255
*Inorg. Chem.* 2019, 58, 7243–7254

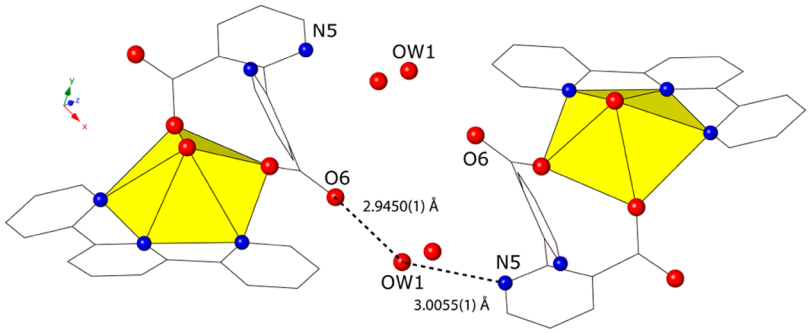


**Figure 2.** Hydrogen bonds link crystallographically equivalent uranyl monomers in **1** through a carboxylate, lattice water molecule, and nitrogen-containing pyridine ring.

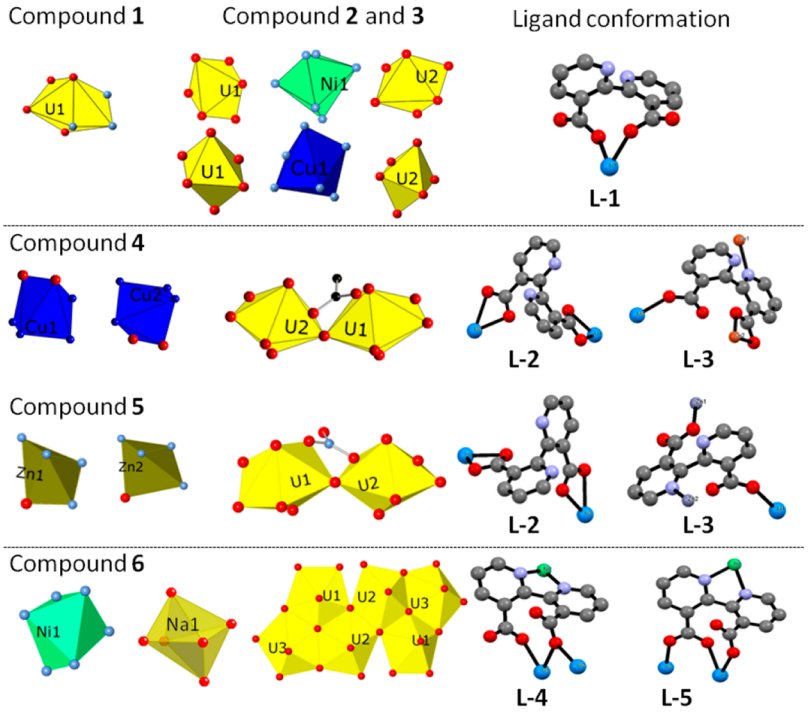


**Figure 3.** Summary of the primary building units (PBUs), secondary building units (SBUs), and binding modes of the **L** ligands in compounds **1**–**6**. In the ball-and-stick figures depicting ligand conformation, blue spheres are uranium atoms, red spheres are oxygen atoms, dark gray spheres are carbon atoms, light blue spheres are nitrogen atoms, orange spheres are copper atoms, light gray spheres are zinc atoms, and green spheres are nickel atoms.

interactions assemble the 1D copper only chains into a 2D supramolecular sheet in the (100) plane (Figure 6). **L-3** coordinates to Cu1 through a nitrogen (N9) at 2.193(8) Å and to Cu2 through the monodentate carboxylate moiety at 1.990(6) Å, whereas the other **L-3** type coordinates Cu1 through the carboxylate group at 2.011(6) Å and to Cu2 by the N4 nitrogen at a distance of 2.221(10) Å. **L-3** ligands also coordinate to U1 and U2, respectively, with a monodentate carboxylate bridge, assembling the copper only 2D sheets with the uranyl only 1D chains into a 3D MOF (Figure 6). The connectivities displayed by the organic ligands and inorganic metal centers in **4** and **5** may be classified as $I^0O^3$ nets where $O^3$ denotes a 3D framework through the organic **L** linkers' connection to multiple metal centers, classifying these compounds as MOFs.

Compound **6** crystallizes in the tetragonal space group $I4_1/acd$ and is unique with respect to the other compounds discussed thus far. A hexameric uranyl unit, generated via three unique pentagonal bipyramidal uranyl metal centers and an inversion center, is coordinated to six symmetrically equivalent nickel units that consist of a $Ni^{2+}$ metal center chelated by two unique **L** ligands (**L-4** and **L-5** conformers, respectively) (Figure 7). Nine unique water molecules and a sodium ion (Na1) are also in the lattice. U1 is coordinated by a $\mu_3$-bridging oxide (U1–O7: 2.207(11) Å), a $\mu_3$-bridging hydroxide (U1–O8: 2.249(10) Å), a monodentate carboxylate (U1–O16: 2.429(11) Å), a $\mu_2$-bridging monodentate carboxylate (U1–O17: 2.487(8) Å), and a bidentate carboxylate (U1–O14: 2.393(8) Å) which bridges to U2 through O13 (2.456(11) Å). U2 is further coordinated by two symmetry equivalent $\mu_3$-bridging hydroxides (U2–O8: 2.257(8) Å), a $\mu_3$-bridging oxide (U2–O7: 2.275(10) Å), and a $\mu_2$-bridging monodentate carboxylate (U2–O9: 2.548(8) Å) which coordinates to U3 through a bond distance of 2.510(9) Å. Completing the hexameric unit, U3 is bound by a $\mu_3$-bridging oxide (U3–O7: 2.171(9) Å), two monodentate carboxylates (U3–O11: Å and U3–O19: Å), and a $\mu_2$-bridging monodentate carboxylate (U3–O17: 2.488(11) Å). The **L**


DOI: 10.1021/acs.inorgchem.9b00255
*Inorg. Chem.* 2019, 58, 7243–7254

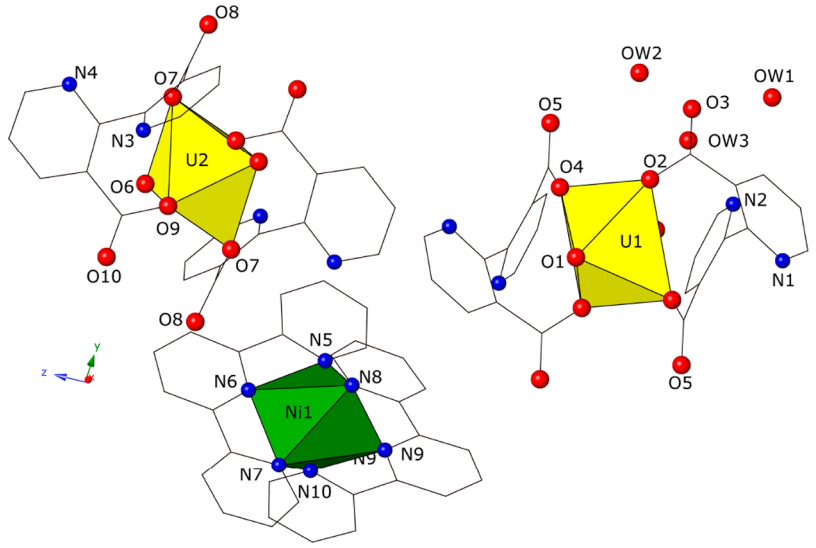


**Figure 4.** Polyhedral representation of the asymmetric unit of compound **2**. Green polyhedral represent nickel metal centers.

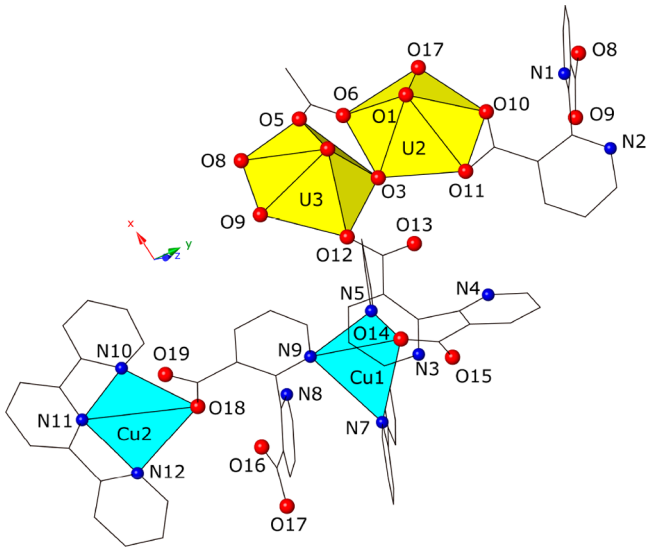


**Figure 5.** Polyhedral representation of the asymmetric unit of compound **4**. Light blue polyhedra represent copper centers. Lattice water molecules have been removed for clarity.

ligands coordinate the nickel metal center at a Ni−N bond distance range of 2.05(1)−2.13(1) Å.

A notable feature to highlight in compound **6** is the large 1D cylindrical channels along [001] (denoted with an "A" in Figure 8). The diameter of these channels, measured between two nickel atoms (Ni1−Ni1) using the Mercury program, is approximately 19.6 Å, which is smaller than the 27 Å pores reported for the NU-1300 uranyl material presented by Farha et al. recently.[25] Additionally, a smaller channel in the same direction as A, denoted as B, has a diameter of 5.6 Å and contains $Na^+$ cations surrounded by oxygens belonging to **L** ligands, exhibiting a distorted octahedral geometry (Figure 8). The void volume of the principal channels is 20696 $Å^3$, whereas a total volume of 21 008 $Å^3$ was calculated taking into account all the small pores (sizes in the 8−16 $Å^3$ range) within the rest of the framework. Despite the large pore size, BET analysis found a surface area of 11 $m^2/g$ (SI, Figure S25). Selected bond distances of all compounds (**1**−**6**) are given in Table S2, and bond valence values are provided in Table S3 in the SI.

**3.2. Thermal Properties of Compound 6.** Thermogravimetric analysis on **6** found a relatively high thermal stability, with complete degradation of the MOF occurring after 300 °C (Figure S14). Initial mass loss from the compound is attributed to water molecules in the pores of the MOF, losing 10.9% mass between 30 and 100 °C, corresponding to approximately 10−11 $H_2O$ molecules per formula unit. Significant mass loss occurs after 300 °C (36.24%) which corresponds to loss of a majority of the organic ligand (37.8%). Many MOFs are reported to have a thermal stability regime that is comparable to that of compound **6** (300−400 °C), whereas some are more stable to slightly higher temperatures, e.g., NU-1300, UiO-66, and ZIFs (400−550 °C).[26] Also, as seen in Figure S15, the initial dehydration process up to 150 °C facilitated a partial loss of crystallinity as evidenced by a PXRD pattern collected after an incomplete thermal degradation (see section III in the SI).

**3.3. Topological Analysis.** Obtaining the underlying topology of a framework structure allows one to describe the compound in the context of the associated net.[27] Related materials may be analyzed and simplified in order to classify and more easily understand the resultant global structural features. The obtained nets of a given topological analysis are classified considering the ideal nets present in the Reticular Chemistry Structure Resource Database and a three letter code symbol such as **abc**, or a symbol with extensions such as abc-d, is assigned.[28] A topological analysis with the TOPOS program[29] found that compounds **1**, **2**, **3** and **4**, **5** share the same topological structure, respectively, and that **6** represents a novel net designated here as **geg1**. Topology results are summarized in Table 2.

An additional analysis, the cluster simplification procedure implemented in ToposPro, allows one to identify the more complex building blocks of a structure and characterize their connection mode. Cluster simplification identifies finite fragments of the structure (its building blocks), the coordination bonds (metal−ligand bonds) within fragments, and coordination bonds that assemble fragments together. As a rule, only coordination bonds are considered in the assembly of a structure from the building block fragments. According to


DOI: 10.1021/acs.inorgchem.9b00255
Inorg. Chem. 2019, 58, 7243−7254

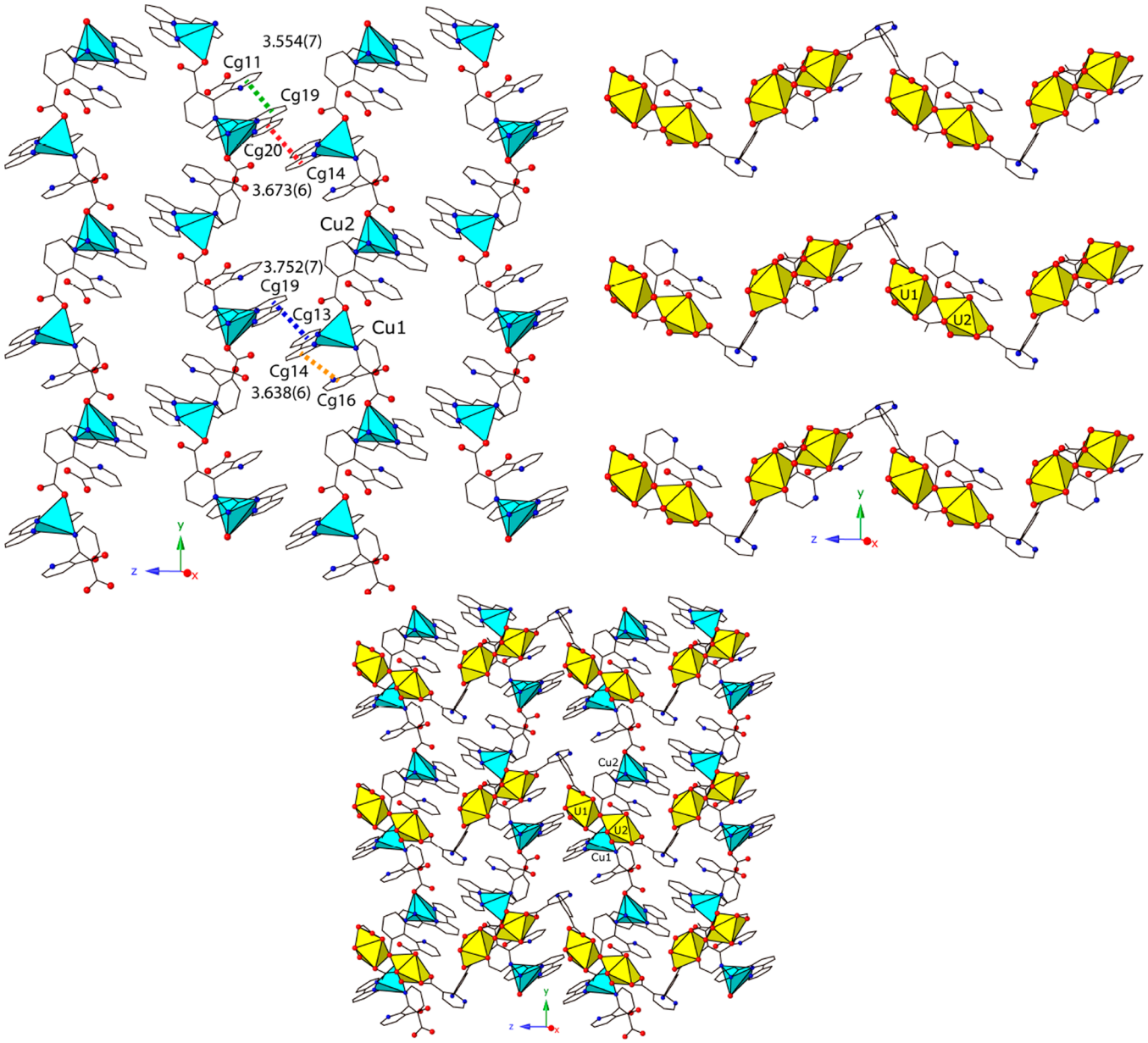


**Figure 6.** Polyhedral representations of compound **4** that show two homometallic 1D chains in the [010] ($Cu^{2+}$, top left) and [001] ([$UO_2^{2+}$], top right) directions. Homometallic sets of chains in the (100) plane alternate to form a covalently bonded 3D framework (bottom). Offset $\pi$-stacking interactions are also observed between $Cu^{2+}$ 1D chains (top left).

the cluster analysis, the structure of compound **6** contains cluster fragments of two species that have a composition of $U_6C_2O_{24}$ and $NiC_{30}H_{17}N_6$ (Figure 9a). These fragments are bonded together by carboxylate groups of the **L** ligand (O and CO fragments). Two Ni-containing fragments are bonded to a U-containing fragment through three coordination bonds. Four Ni-containing fragments are bonded to a U-containing fragment through two coordination bonds (these bonds are shown in the Figure 9a with a dotted line).

To determine the underlying net, the cluster fragments contract to their geometric centers of gravity; the result of this operation is depicted in the Figure 9b. The subsequent secondary simplification of the net includes removal of the 0- and 1-coordinated nodes (extraframework and terminal structural groups) and replacing the 2-coordinated nodes (bridge structural groups) by net edges. The cluster representation of the structure resulted in the underlying net of the **geg1** topological type (Figure 9c). Compound **6** represents the first known occurrence of the **geg1** type, and it displays two distinct channels that run in the [001] direction. Four bands of quadrangular rings border a wide channel (Figure 9d, top), whereas octagonal rings (Figure 9d, bottom) form a narrow channel. Taking into account the different type of ligand coordination to uranium atoms, we can assemble several fragments into one larger, aggregated fragment, or "union" fragment, that has the composition $U_6Ni_2C_{64}H_{34}N_{12}O_{28}$ (Figure 10a). If such fragments are considered as clusters during the Topos simplification process, then we obtain an underlying net of topological type **sqc2077** and consisting of alternating right and left spirals which are connected together (Figure 10b). This net is rare but has an analogous example in the literature as a standard representation of the H-bond containing molecular structure $[Co(H_2PIDC)_2(H_2O)_2]$,[30]



DOI: 10.1021/acs.inorgchem.9b00255
*Inorg. Chem.* 2019, 58, 7243−7254

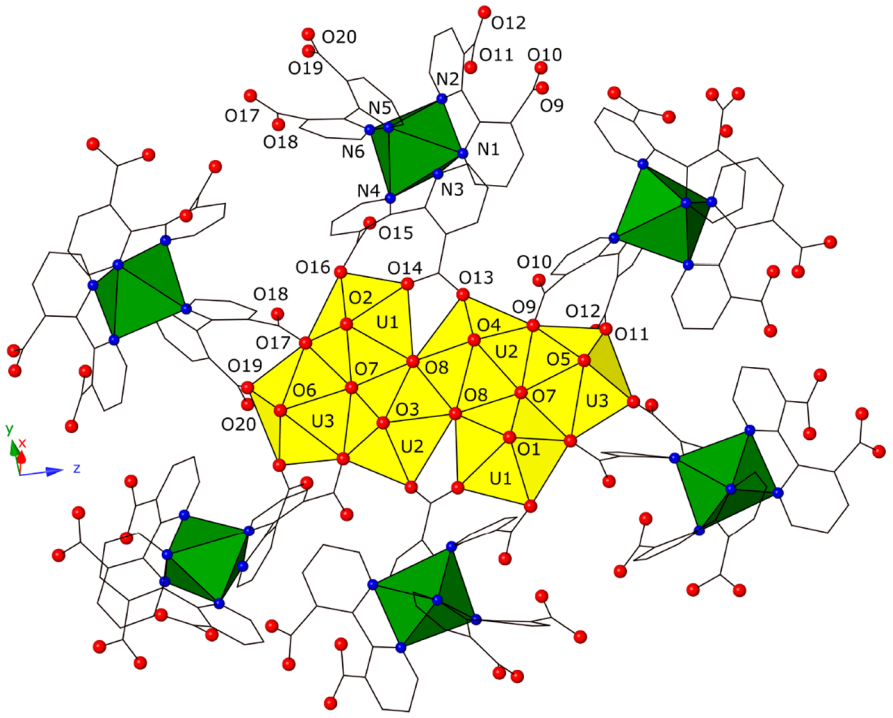


**Figure 7.** Polyhedral representation of compound **6**. A hexameric uranyl unit is coordinated to six symmetrically equivalent nickel units. Lattice water molecules and a sodium ion have been removed for clarity.

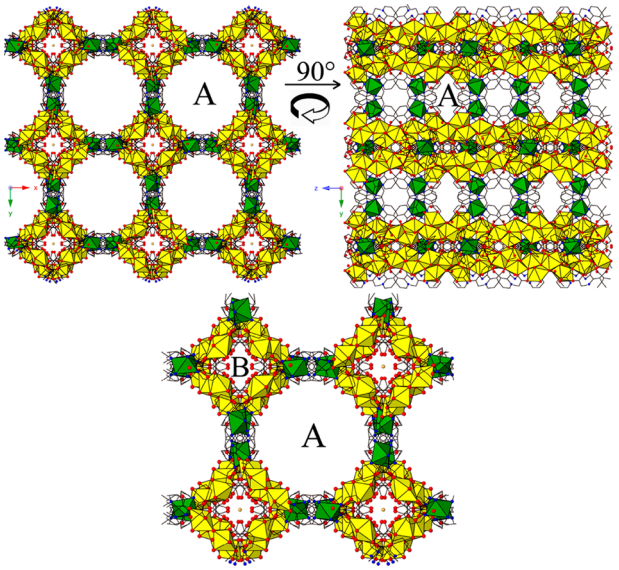


**Figure 8.** Compound **6** viewed down the [001] (left) and [100] (right) directions with an enlarged view showing the A and B channels (bottom).

where PIDC is 2-propyl-5-carboxy-1*H*-imidazole-4-carboxylate.

## 4. STRUCTURAL DISCUSSION

The linear nature of the $[UO_2]^{2+}$ cation and the nominally terminal behavior of the "yl" oxygen atoms create a propensity for equatorial coordination and favor the formation of 1D and 2D coordination polymers.[8,31] In an effort to explore 3D uranyl materials, many studies have employed polytopic ligands as a strategy to generate higher order architectures and new topologies.[5] For example, Farha et al. employed nonplanar organic ligands such as the pseudo-four-fold symmetric linker 4,4′,4′′,4′′′-(pyrene-1,3,6,8-tetryl)tetrabenzoic acid ($H_4$TBAPy)[24] to generate a noninterpenetrated uranyl-containing MOF with a *tbo* topology and large open cavities (17, 24, and 39 Å) and by using the tritopic 5′-(4-carboxyphenyl)-2′,4′,6′-trimethyl-[1,1′:3′,1′′-terphenyl]-4,4′′-dicarboxylic acid[32] ligand to form a mesoporous U-MOF containing large icosidodecahedral cavities with internal diameters of 50 and 62 Å. Another example, reported by Shi et al.,[33] details the assembly of actinides through carboxylates and $Ag^+$ ions to form the 3D compounds $[Ag(UO_2)_2(\mu_2\text{-}OH)(\mathbf{L})_2(H_2O)_2]$ and $[Ag_3Th_6(\mu_3\text{-}O)(\mu_3\text{-}OH)(\mu_2\text{-}OH)_6(\mathbf{L})_6(NO_3)_6{\cdot}H_2O]$. Therein, the nitrogen atoms of the pyridine rings coordinated to the $Ag^+$ metal center, and the carboxylates coordinated to the actinides, to provide additional bonding to increase framework dimensionality. In the present study, the 2,2′-bipyridine-3,3′-dicarboxylic acid ($\mathbf{H_2L}$) was employed as the polytopic ligand as it exhibits several moieties where coordination to a metal center is possible, carboxylates and nitrogens from the bipyridine rings.

Others have utilized d- or f-block metal centers to generate high dimensionality frameworks. Shi and colleagues[34] have synthesized a set of bimetallic frameworks with 2,2′-bipyridine-4,4′-dicarboxylic acid encompassing a variety of structures, several of which are 3D frameworks ($UO_2$-Zn, $UO_2$-Cu, and $UO_2$-Co). As such, our approaches herein are consistent with those of others that have resulted in 3D structures, specifically with respect to polytypic ligands and d-metals.

When the $[UO_2]^{2+}$ cation was combined with the $\mathbf{H_2L}$ ligand in the absence of secondary metals, in a study by Thuéry and Masci, a set of 1D chain structures was obtained:[35] $[UO_2(\mathbf{L})(H_2O)]{\cdot}3H_2O$, $[UO_2(\mathbf{L})(DMF)]{\cdot}0.5H_2O$, and $[UO_2(\mathbf{L})(H_2\mathbf{L})]{\cdot}H_2O$, reinforcing the tendency of $[UO_2]^{2+}$ to generate low dimensional compounds. In our case, the combination of $\mathbf{H_2L}$ and **TPY** with $[UO_2]^{2+}$ leads to a 0D


DOI: 10.1021/acs.inorgchem.9b00255
*Inorg. Chem.* 2019, 58, 7243−7254

**Table 2. Summary of Topological Analysis of Actinide-Based CPs, Including Compounds 1−6**

| compound | dimensionality ($I^nO^m$) | cell vol (Å$^3$) | void volume (Å$^3$)[a] | nodality | standard representation | cluster representation | ref |
|---|---|---|---|---|---|---|---|
| **1** | 0D ($I^0O^0$) | 1277.98(7) | | 2 | 1,4M5-1 | | this study |
| **2** | 0D ($I^0O^0$) | 2554.75(13) | | 2 | 1,4M5-1 | | this study |
| **3** | 0D ($I^0O^0$) | 2578.3(9) | | 2 | 1,4M5-1 | | this study |
| **4** | 3D ($I^0O^3$) | 7177.8(10) | | 1 | ths ThSi2; 3/10/t4 | **tfc** | this study |
| **5** | 3D ($I^0O^3$) | 7205.7(18) | | 1 | ths ThSi2; 3/10/t4 | **tfc** | this study |
| **6** | 3D ($I^0O^3$) | 57689(10) | 21008 | 9 | 3,3,3,3,3,3,3,4,5-c net | novel type: **geg1** | this study |
| $[UO_2(\mathbf{L})(H_2O)]\cdot 3H_2O$ | 1D ($I^1O^0$) | 866.81(17) | | 2 | ($4^2$,6) | | ref 36 |
| $[UO_2(\mathbf{L})(DMF)]\cdot 0.5H_2O$ | 1D ($I^1O^0$) | 870.70(10) | | 2 | ($4^2$,6) | | ref 36 |
| $[UO_2(\mathbf{L})(H_2\mathbf{L})]\cdot H_2O$ | 1D ($I^1O^0$) | 2421.0(3) | | 2 | ($4^2$,6) | | ref 36 |
| $[Ag(UO_2)_2(\mu_2\text{-}OH)(\mathbf{L})_2(H_2O)_2]$ | 3D ($I^0O^3$) | 11503.3(7) | no accessible void[b] | | not reported | | ref 34 |
| $[Ag_3Th_6(\mu_3\text{-}O)(\mu_3\text{-}OH)(\mu_2\text{-}OH)_6(\mathbf{L})_6(NO_3)_6\cdot H_2O]$ | 3D ($I^0O^3$) | 6834.1(15) | 235.9[b] | | not reported | | ref 34 |

[a]Calculated with Platon.[38] [b]Calculated by us in this study.

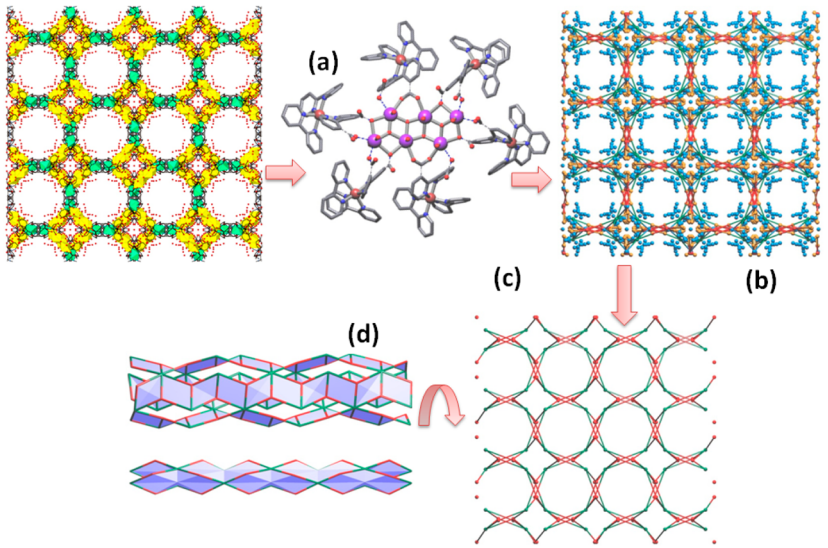


**Figure 9.** Cluster fragments $NiC_{30}H_{17}N_6$ and $U_6C_2O_{24}$ of compound **6** (a). Hydrogen atoms are omitted for clarity. Cluster representation of the coordination polymer and the net obtained after primary simplification (b). The 3,6-c underlying net of **geg1** topological type obtained after secondary simplification procedure (c). The **geg1** net contains wide (d, top) and narrow (d, bottom) channels.

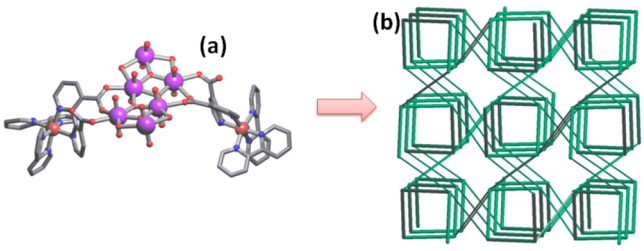


**Figure 10.** A union fragment can be constructed from three cluster fragments (a). Hydrogen atoms are omitted for clarity. Net with topology **sqc2077** built from infinite spirals (b).

molecular structure (**1**). The addition of $Cu^{2+}$ and $Ni^{2+}$ in a 0.5:1 ratio with respect to $[UO_2]^{2+}$ cation in the synthesis of **2** and **3** compounds produces 0D species as well, due to the chelation and encapsulation of the transition metals by two **TPY** molecules. Uranyl units are exclusively bounded by **L** ligands. This phenomenon is an example of the coordination preferences exhibited by the uranyl and d-metals according to HSAB preferences that essentially gave rise to a "phase separation" on a molecular level.[11] When the $Cu^{2+}$:$[UO_2]^{2+}$ or $Zn^{2+}$:$[UO_2]^{2+}$ ratio is increased to 1:1, compounds **4** and **5** are generated and the coordination of $Cu^{2+}$ or $Zn^{2+}$ by **TPY** is maintained and the **L** linkers further coordinate the transition metal and uranyl ions together to generate 3D frameworks. Increasing the molar ratio of $UO_2^{2+}$ to $Ni^{2+}$ to 3:1 produces single crystals of compound **6**, wherein, coincidently, a 3:1 uranium-to-nickel ratio is maintained in the crystal structure.

Metal ion hydrolysis is readily apparent in compounds **4**−**5** and **6** where hydroxide bridged uranyl dimers and a uranyl hexamer are observed. Hydrolysis of $[UO_2]^{2+}$ cations in solution, demonstrated within the uranyl hydrolysis equation (1), is quite common in hydrothermal syntheses and can produce significantly oligomerized units through the creation of point-shared, bridging hydroxo- ($OH^-$, hydroxylation) or


DOI: 10.1021/acs.inorgchem.9b00255
Inorg. Chem. 2019, 58, 7243−7254

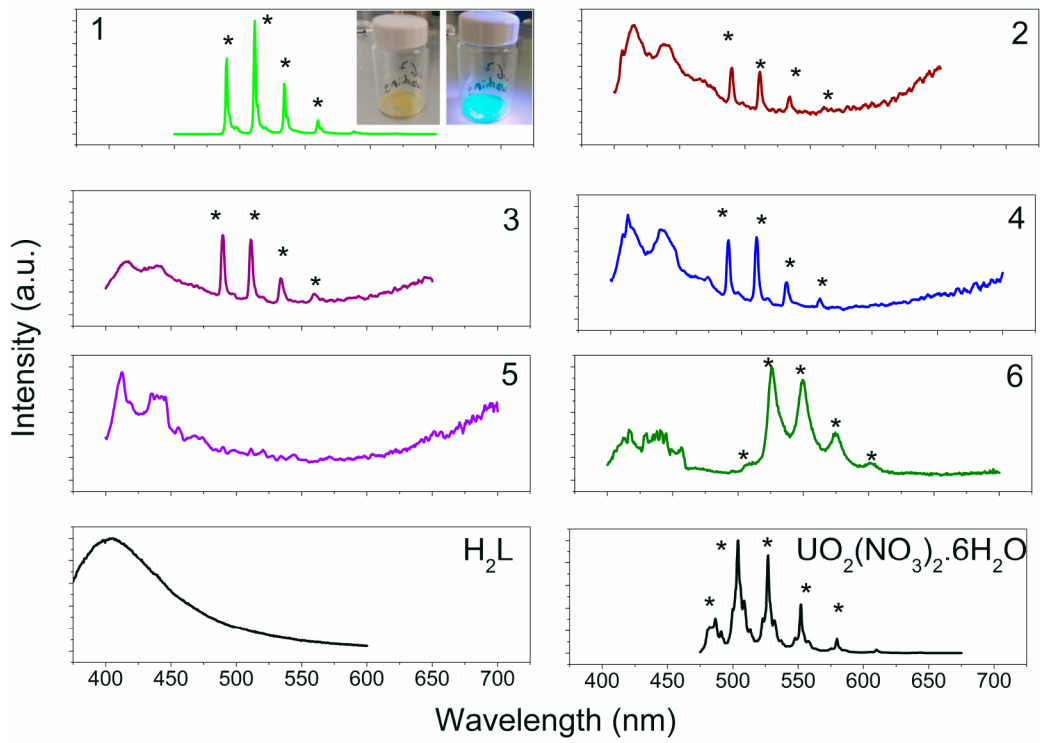


**Figure 11.** Emission spectra of compounds **1**–**6** ($\lambda_{exc}$ = 365 nm), collected at approximately 77 K, compared to the luminescent emission from $UO_2(NO_3)_2{\cdot}6H_2O$ and **$H_2$L**. The asterisks mark the uranyl transitions. The inset in the spectrum of compound **1** shows the sample before and during of UV light exposure.

oxo- ($O^{2-}$, oxolation) groups.[36] According to the uranyl hydrolysis equation, oligomerization of the uranyl cation into more condensed species is influenced by both higher $[UO_2]^{2+}$ concentrations and pH, with larger units prevalent at pH values above 4.5.[37] The pH of the reactions herein were adjusted to approximately 5, which may have assisted in the formation of dimers (**4** and **5**) and hexamers (**6**). All compounds featuring oligomerized uranyl species were also 3D structures, perhaps suggesting oligomerization, at least in this system, is a prerequisite for MOF formation.

$$m[UO_2]^{2+} + nH_2O \rightleftarrows (UO_2)_m(OH)_n^{2m-n} + nH^+ \qquad (1)$$

## 5. SOLID STATE PHOTOLUMINESCENCE (SSPL) PROPERTIES

Collecting emission spectra and time-resolved luminescent lifetimes ($\tau_{obs}$) is a notable way to elucidate information about the luminescent behavior of metal-content materials,[2] all of which can be informative when exploring structure–property relationships. Uranyl luminescent emission originates from a ligand to metal charge transfer (LMCT) that excites an electron from nonbonding $5f_\delta$, $5f_\varphi$ uranyl orbitals to uranyl–oxygen bonding orbitals ($\sigma_u$, $\sigma_g$, $\pi_u$, $\pi_g$),[39] which is further coupled to "yl" vibrational ($S_{11} \rightarrow S_{01}$ and $S_{10} \rightarrow S_0\nu$ [$\nu$ = 0–4]) states of the U═O axial bond.[40] This luminescence is characterized by green emission, often observed as four to six vibronically coupled peaks in the 400–650 nm range. We have explored the SSPL properties of all six compounds by exciting into the LMCT band with incident light at 365 nm (Figure 11). All compounds are compared to the emission spectra of uranyl nitrate ($UO_2(NO_3)_2{\cdot}6H_2O$) and the **$H_2$L** free ligand. A summary of the SSPL properties of compounds **1**–**6** is provided in section IX in the SI.

In compounds **1**–**4**, a red shift of between 7 and 8 nm, with respect to the luminescence of $UO_2(NO_3)_2{\cdot}6H_2O$, is observed. Shifts in the position of uranyl can arise from changes in the coordination environment of the uranyl metal center,[41] and recent efforts have shown that chelation by nitrogen-containing electron donating ligands may have a red-shift effect on the emission spectrum as well.[42] For compounds **2**, **3**, and **4**, similar spectra are obtained demonstrating classic uranyl emission accompanied by broad ligand bands (400–475 nm) emissions. Compound **5** shows no evidence of uranyl emission, which may be attributed to efficient quenching through nonradiative pathways through d-block metals.[8b,43]

The luminescence lifetime ($\tau_{obs}$) of uranyl bearing materials can also provide information about the surrounding environment, both locally (direct coordination to uranyl metal center) and globally (e.g., lattice water molecules outside of the first coordination sphere). The uranyl $\tau_{obs}$ partially depends on the presence of quenching molecules or atoms close to the $[UO_2]^{2+}$ moiety, where shorter lifetimes are an indication of increased quenching.[44] Excited $[UO_2]^{2+}$ species typically decay monoexponentially, yet a multiexponential luminescence decay frequently indicates the presence of more than one luminescent center in the compound.[44] As detailed in sections VIII and IX in the SI, the $\tau_{obs}$ of all compounds vary with structure. Time resolved luminescent data on **1** finds a long-lived lifetime ($\tau_{obs}$ = 0.979 ms) and a monoexponential fit, likely corresponding to a single emitting species. The decay profiles of the isostructural compounds **2** and **3** are best fitted by monoexponentials with $\tau_{obs}$ values of 0.057 and 0.0413 ms, respectively. The presence of a number of lattice water molecules and the incorporation of transition metals may


DOI: 10.1021/acs.inorgchem.9b00255
Inorg. Chem. 2019, 58, 7243–7254

provide quenching pathways and perhaps explain the shorter lifetimes.[45] Compound **4** exhibits a decay profile with a biexponential fitting, finding two lifetimes of 0.02 and 0.0796 ms, which is consistent with the presence of two emitting centers. The SSPL properties of compound **6** deserve particular attention owing to the uniqueness of its structure and the luminescence properties observed. First, the emission spectrum exhibits a well-structured uranyl signature, with higher intensity compared to the ligand co-emission. The spectrum is significantly red-shifted (by 21.5 nm) with respect to the uranyl nitrate salt, and the peaks are broader when compared to the other compounds in this study. These features may arise from the significant oligomerization, which has been shown to red-shift uranyl emission.[46] The decay could be fit with a biexponential model with lifetime values of 0.0056 and 0.093 ms. Although we hesitate to comment on a well-defined luminescent lifetime trend across the five compounds (**1**−**4**, and **6**), owing to the variation in uranyl and secondary metal center local coordination spheres, we do observe significantly decreased lifetimes in compounds which contain a secondary transition metal center.

## 6. CONCLUSIONS

Six new $UO_2^{2+}$-containing compounds utilizing the 2,2′-bipyridine-3,3′-dicarboxylic acid ligand (**$H_2$L**) have been synthesized under solvothermal conditions and characterized by single-crystal and powder X-ray diffraction. The compounds can be categorized into two groups based upon structural dimensionality: three 0D molecular units ([$(UO_2)$(**L**)(**TPY**)]·$H_2O$ (**1**), [Ni(**TPY**)$_2$][$(UO_2)$(**L**)$_2$]·3$H_2O$ (**2**), and [Cu(**TPY**)$_2$][$(UO_2)$(**L**)$_2$]·3$H_2O$ (**3**)) and three 3D MOFs ([$Cu_2$($(UO_2)_2$(OH)(OAc)(**L**)$_3$(**TPY**)$_2$]·(2-propanol)·6$H_2O$ (**4**), [$Zn_2$($UO2)_2$(OH)($NO_3$)(**L**)$_3$(**TPY**)$_2$]·4$H_2O$ (**5**), and Na[Ni($(UO_2)_3$(OH)(O)(**L**)$_3$]·9$H_2O$ (**6**). Topological analyses elucidated the simplified 2-nodal nets 1,4M5-1, 1,4M5-1, and 1,2M3-1 nets for compounds **1**, **2**, and **3**, respectively, one-nodal ths this2; 3/10/t4 nets for compounds **4** and **5**, and a new **geg1** topology, the 9-nodal 3,3,3,3,3,3,3,4,5-c net, for compound **6**. Most compounds explored herein exhibit characteristic green uranyl emission accompanied by ligand co-emission. In compound **6**, there is a significant red-shifting and transition broadening, likely due to the existence of the oligomerized uranyl hexamer. Thermogravimetric analysis found a relatively high thermal stability of 300 °C for compound **6**. The potential for this uranyl material to absorb different solvents or gases, as well as to perform useful photocatalytic reactions, is an area of active inquiry.

## ■ ASSOCIATED CONTENT

### Supporting Information

The Supporting Information is available free of charge on the ACS Publications website at DOI: 10.1021/acs.inorgchem.9b00255.

Reaction conditions, ORTEP thermal ellipsoid plots, PXRD patterns, tables of selected bond distances, luminescent decay lifetime fittings, and BET surface area measurements are provided in the SI (PDF)

### Accession Codes

CCDC 1868282−1868287 contain the supplementary crystallographic data for this paper. These data can be obtained free of charge via www.ccdc.cam.ac.uk/data_request/cif, or by emailing data_request@ccdc.cam.ac.uk, or by contacting The Cambridge Crystallographic Data Centre, 12 Union Road, Cambridge CB2 1EZ, UK; fax: +44 1223 336033.

## ■ AUTHOR INFORMATION


### Corresponding Author

*E-mail: cahill@gwu.edu.

### ORCID

Christopher L. Cahill: 0000-0002-2015-3595


### Notes

The authors declare no competing financial interest.

## ■ ACKNOWLEDGMENTS

This study was supported by the U.S. Department of Energy (DOE) - Chemical Sciences, Geosciences and Biosciences Division, Office of Science, Office of Basic Energy Sciences, Heavy Elements Program, under grant number DE-FG02-05ER15736. G.E.G. is member of CIC-CONICET (Carrera del Investigador Científico-Consejo Nacional de Investigaciones Científicas y Técnicas) and thanks the Fulbright Program for supporting his visit to GW.

## ■ REFERENCES


(1) Rosi, N. L.; Eckert, J.; Eddaoudi, M.; Vodak, D. T.; Kim, J.; O'keeffe, M.; Yaghi, O. M. Hydrogen storage in microporous metal-organic frameworks. *Science* **2003**, *300*, 1127−1129.

(2) Heine, J.; Müller-Buschbaum, K. Engineering metal-based luminescence in coordination polymers and metal−organic frameworks. *Chem. Soc. Rev.* **2013**, *42*, 9232−9242.

(3) (a) Wang, J.-L.; Wang, C.; Lin, W. Metal-organic frameworks for harvesting and photocatalysis. *ACS Catal.* **2012**, *2*, 2630−2640. (b) Corma, A.; García, H.; Llabrés i Xamena, F. X. Engineering metal organic frameworks for heterogeneous catalysis. *Chem. Rev.* **2010**, *110*, 4606−4655.

(4) (a) Su, J.; Chen, J. S. MOFs of Uranium and the Actinides. *Struct. Bonding (Berlin, Ger.)* **2014**, *163*, 265−296. (b) Andrews, M. B.; Cahill, C. L. Uranyl Bearing Hybrid Materials: Synthesis, Speciation, and Solid-State Structures. *Chem. Rev.* **2013**, *113*, 1121−1136. (c) Loiseau, T.; Mihalcea, I.; Henry, N.; Volkringer, C. The crystal chemistry of uranium carboxylates. *Coord. Chem. Rev.* **2014**, *266*, 69−109. (d) Yang, W.; Parker, T. G.; Sun, Z. M. Structural chemistry of uranium phosphonates. *Coord. Chem. Rev.* **2015**, *303*, 86−109.

(5) Thuéry, P.; Harrowfield, J. Recent advances in structural studies of heterometallic uranyl-containing coordination polymers and polynuclear closed species. *Dalton Trans.* **2017**, *46*, 13660−13667.

(6) (a) Natrajan, L. S. Developments in the photophysics and photochemistry of actinide ions and their coordination compounds. *Coord. Chem. Rev.* **2012**, *256*, 1583−1603. (b) Yang, W.; Bai, Z.-Q.; Shi, W.-Q.; Yuan, L.-Y.; Tian, T.; Chai, Z.-F.; Wang, H.; Sun, Z.-M. MOF-76: from a luminescent probe to highly efficient $U^{VI}$ sorption material. *Chem. Commun.* **2013**, *49*, 10415−10417. (c) Xia, Y.; Wang, K.-X.; Chen, J.-S. Synthesis, structure characterization and photocatalytic properties of two new uranyl naphthalene-dicarboxylate coordination polymer compounds. *Inorg. Chem. Commun.* **2010**, *13*, 1542−1547. (d) Hou, Y.-N.; Xing, Y.-H.; Bai, F.-Y.; Guan, Q.-L.; Wang, X.; Zhang, R.; Shi, Z. Synthesis, crystal structure, photoluminescence property and photoelectronic behavior of two uranyl-organic frameworks constructed from 1, 2, 4, 5-benzenetetracarboxylic acid as ligand. *Spectrochim. Acta, Part A* **2014**, *123*, 267−272.

(7) (a) Thuéry, P.; Harrowfield, J. Tetrahedral and Cuboidal Clusters in Complexes of Uranyl and Alkali or Alkaline-Earth Metal Ions with rac- and (1R,2R)-trans-1,2-Cyclohexanedicarboxylate. *Cryst. Growth Des.* **2017**, *17*, 2881−2892. (b) Adelani, P. O.; Albrecht-Schmitt, T. E. Metal-controlled assembly of uranyl diphosphonates toward the design of functional uranyl nanotubules. *Inorg. Chem.* **2011**, *50*, 12184−12191. (c) Mihalcea, I.; Henry, N.; Loiseau, T.




DOI: 10.1021/acs.inorgchem.9b00255
*Inorg. Chem.* 2019, 58, 7243−7254

Revisiting the Uranyl-phthalate System: Isolation and Crystal Structures of Two Types of Uranyl−Organic Frameworks (UOF). *Cryst. Growth Des.* **2011**, *11*, 1940−1947. (d) Falaise, C.; Volkringer, C.; Vigier, J.-F.; Beaurain, A.; Roussel, P.; Rabu, P.; Loiseau, T. Isolation of the Large $\{Actinide\}_{38}$ Poly-oxo Cluster with Uranium. *J. Am. Chem. Soc.* **2013**, *135*, 15678−15681. (e) Pasquale, S.; Sattin, S.; Escudero-Adán, E. C.; Martínez-Belmonte, M.; de Mendoza, J. Giant regular polyhedra from calixarene carboxylates and uranyl. *Nat. Commun.* **2012**, *3*, 785. (f) Thuéry, P.; Harrowfield, J. Coordination Polymers and Cage-Containing Frameworks in Uranyl Ion Complexes with rac- and (1R,2R)-trans-1,2-Cyclohexanedicarboxylates: Consequences of Chirality. *Inorg. Chem.* **2017**, *56*, 1455−1469. (g) Thuéry, P.; Villiers, C.; Jaud, J.; Ephritikhine, M.; Masci, B. Uranyl-Based Metallamacrocycles: Tri- and Tetranuclear Complexes with (2R,3R,4S,5S)-Tetrahydrofurantetracarboxylic Acid. *J. Am. Chem. Soc.* **2004**, *126*, 6838−6839.

(8) (a) Olchowka, J.; Falaise, C.; Volkringer, C.; Henry, N.; Loiseau, T. Structural Observations of Heterometallic Uranyl Copper (II) Carboxylates and Their Solid State Topotactic Transformation upon Dehydration. *Chem. - Eur. J.* **2013**, *19*, 2012−2022. (b) Thuéry, P.; Harrowfield, J. Chiral one- to three-dimensional uranyl−organic assemblies from (1R,3S)-(+)-camphoric acid. *CrystEngComm* **2014**, *16*, 2996. (c) Thuéry, P.; Harrowfield, J. Uranyl Ion Complexes with trans-3-(3-Pyridyl)acrylic Acid Including a Uranyl-Copper(II) Heterometallic Framework. *Eur. J. Inorg. Chem.* **2014**, *2014*, 4772−4778. (d) Weng, Z.; Zhang, Z. H.; Olds, T.; Sterniczuk, M.; Burns, P. C. Copper(I) and Copper(II) Uranyl Heterometallic Hybrid Materials. *Inorg. Chem.* **2014**, *53*, 7993−7998. (e) Mei, L.; Hu, K-q.; Zhang, Z.-h.; An, S.-w.; Chai, Z.-f.; Shi, W.-q. Stepwise ortho Chlorination of Carboxyl Groups for Promoting Structure Variance of Heterometallic Uranyl-Silver Coordination Polymers of Isonicotinate. *Inorg. Chem.* **2018**, *57*, 4673−4685. (f) Mei, L.; Wu, Q-y.; An, S.-w.; Gao, Z.-q.; Chai, Z.-f.; Shi, W.-q. Silver Ion-Mediated Heterometallic Three-Fold Interpenetrating Uranyl-Organic Framework. *Inorg. Chem.* **2015**, *54*, 10934−10945. (g) Yu, Z.-T.; Liao, Z.-L.; Jiang, Y.-S.; Li, G.-H.; Chen, J.-S. *Chem. - Eur. J.* **2005**, *11*, 2642−2650. (h) Chen, W.; Yuan, H.-M.; Wang, J.-Y.; Liu, Z.-Y.; Xu, J.-J.; Yang, M.; Chen, J.-S. Synthesis, Structure, and Photoelectronic Effects of a Uranium-Zinc-Organic Coordination Polymer Containing Infinite Metal Oxide Sheets. *J. Am. Chem. Soc.* **2003**, *125*, 9266−9267.

(9) (a) Thuéry, P. Uranyl and mixed uranyl−lanthanide complexes with p-sulfonatocalix[4]arene. *CrystEngComm* **2012**, *14*, 6369−6373. (b) Knope, K. E.; de Lill, D. T.; Rowland, C. E.; Cantos, P. M.; de Bettencourt-Dias, A.; Cahill, C. L. Uranyl Sensitization of Samarium(III) Luminescence in a Two-Dimensional Coordination Polymer. *Inorg. Chem.* **2012**, *51*, 201−206. (c) Volkringer, C.; Henry, N.; Grandjean, S.; Loiseau, T. Uranyl and/or Rare-Earth Mellitates in Extended Organic−Inorganic Networks: A Unique Case of Heterometallic Cation−Cation Interaction with UVI═O−LnIII Bonding (Ln = Ce, Nd). *J. Am. Chem. Soc.* **2012**, *134*, 1275−1283. (d) Hou, Y.-N.; Xu, X.-T.; Xing, N.; Bai, F.-Y.; Duan, S.-B.; Sun, Q.; Wei, S.-Y.; Shi, Z.; Zhang, H.-Z.; Xing, Y.-H. Photocatalytic Application of 4f-5f Inorganic-Organic Frameworks: Influence of Lanthanide Contraction on the Structure and Functional Properties of a Series of Uranyl-Lanthanide Complexes. *ChemPlusChem* **2014**, *79*, 1304−1315. (e) Mihalcea, I.; Volkringer, C.; Henry, N.; Loiseau, T. Series of Mixed Uranyl−Lanthanide (Ce, Nd) Organic Coordination Polymers with Aromatic Polycarboxylates Linkers. *Inorg. Chem.* **2012**, *51*, 9610−9618.

(10) (a) Bell, N. L.; Arnold, P. L.; Love, J. B. Controlling uranyl oxo group interactions to group 14 elements using polypyrrolic Schiff-base macrocyclic ligands. *Dalton Trans.* **2016**, *45*, 15902−15909. (b) Thuéry, P.; Harrowfield, J. Tetrahydrofurantetracarboxylic Acid: An Isomerizable Framework-Forming Ligand in Homo- and Heterometallic Complexes with $UO_2^{2}$+, $Ag^{+}$ and $Pb^{2+}$. *Cryst. Growth Des.* **2016**, *16*, 7083−7093. (c) Zegke, M.; Nichol, G. S.; Arnold, P. L.; Love, J. B. Catalytic one-electron reduction of uranyl(VI) to Group 1 uranyl(V) complexes via Al(III) coordination. *Chem. Commun.* **2015**, *51*, 5876−5879. (d) Kalaj, M.; Carter, K. P.; Savchenkov, A. V.; Pyrch, M. M.; Cahill, C. L. Syntheses, Structures, and Comparisons of Heterometallic Uranyl Iodobenzoates with Monovalent Cations. *Inorg. Chem.* **2017**, *56*, 9156−9168. (e) Thuéry, P.; Harrowfield, J. $Ag^{I}$ and $Pb^{II}$ as Additional Assembling Cations in Uranyl Coordination Polymers and Frameworks. *Cryst. Growth Des.* **2017**, *17*, 2116−2130.

(11) (a) Thuéry, P.; Harrowfield, J. Three Different Modes of Association between Metal Cations in Heterometallic Uranyl-Co III and Uranyl-Mn II Species. *Eur. J. Inorg. Chem.* **2018**, *2018*, 4465−4471. (b) Liu, K.; Zhou, J.-M.; Li, H.-M.; Xu, N.; Cheng, P. A Series of $Cu^{II}$−$Ln^{III}$ Metal−Organic Frameworks Based on 2,2′-Bipyridine-3,3′-dicarboxylic Acid: Syntheses, Structures, and Magnetic Properties. *Cryst. Growth Des.* **2014**, *14*, 6409−6420. (c) Zhou, J.-M.; Shi, W.; Xu, N.; Cheng, P. A New Family of 4f-3d Heterometallic Metal−Organic Frameworks with 2,2′-Bipyridine-3,3′-dicarboxylic Acid: Syntheses, Structures and Magnetic Properties. *Cryst. Growth Des.* **2013**, *13*, 1218−1225. (d) Zhou, Y.; Li, X.; Zhang, L.; Guo, Y.; Shi, Z. 3-D Silver(I)—Lanthanide(III) Heterometallic-Organic Frameworks Constructed from 2,2′-Bipyridine-3,3′-dicarboxylic Acid: Synthesis, Structure, Photoluminescence, and Their Remarkable Thermostability. *Inorg. Chem.* **2014**, *53*, 3362−3370.

(12) (a) Zhou, J.-M.; Shi, W.; Xu, N.; Cheng, P. Highly selective luminescent sensing of fluoride and organic small-molecule pollutants based on novel lanthanide metal−organic frameworks. *Inorg. Chem.* **2013**, *52*, 8082−8090. (b) Hu, M.; Li, H.-F.; Yao, J.-Y.; Gao, Y.; Liu, Z.-L.; Su, H.-Q. Hydrothermal synthesis and characterization of two 2-D lanthanide-2,2'-bipyridine-3,3'-dicarboxylate coordination polymers based on zigzag chains. *Inorg. Chim. Acta* **2010**, *363*, 368−374. (c) Zhong, Z. J.; You, X.-Z.; Yang, Q.-C. Crystal structure and properties of a polymeric chain copper(II) complex $[Cu(bpc)(H_2O)_2]$ (bpc = 2,2′-bipyridyl-3,3′-dicarboxylate). *Polyhedron* **1994**, *13*, 1951−1955. (d) Chen, X.-L.; Yao, Y.-J.; Hu, H.-M.; Chen, S.-H.; Fu, F. Synthesis, structure, and characterization of a silver(I) coordination polymer with $\mu$6-bridging 2,2′-bipyridyl-3,3′-dicarboxylate. *J. Coord. Chem.* **2009**, *62*, 2147−2154. (e) Modanlou Juibari, N.; Abbasi, A.; Hasani, N. Hydrothermal synthesis of novel cobalt−organic framework, involving in-situ ligand transformation, DFT calculation, spectroscopic and thermal studies. *Inorg. Chim. Acta* **2015**, *432*, 267−274. (f) Sun, J.-Y.; Wang, W.; Wang, L.; Zhang, D.-J.; Chen, Y.-L.; Ji, X.-D.; Fan, Y.; Song, T.-Y. Novel lead-organic framework based on 2,2′-bipyridine-3,3′-dicarboxylate ligand: Synthesis, structure and luminescence. *J. Mol. Struct.* **2011**, *990*, 204−208. (g) Wu, B.; Yuan, D.; Jiang, F.; Wang, R.; Han, L.; Zhou, Y.; Hong, M. Metal Directed Self Assembly: Two New Metal Binicotinate Grid Polymeric Networks and Their Fluorescence Emission Tuned by Ligand Configuration. *Eur. J. Inorg. Chem.* **2004**, *2004*, 2695−2700. (h) Wu, B.-L.; Zhang, H.-Q.; Zhang, H.-Y.; Wu, Q.-A.; Hou, H.-W.; Zhu, Y.; Wang, X.-Y. Unique Tetradentate Coordination of 2,2′-Bipyridyl-3,3′-Dicarboxylate (bpdc). Hydrothermal Synthesis and Crystal Structure of A Novel Polymeric Supramolecule $[Co(bpdc)(H_2O)_2]_n$. *Aust. J. Chem.* **2003**, *56*, 335−338.

(13) (a) Thangavelu, S. G.; Pope, S. J. A.; Cahill, C. L. Synthetic, structural, and luminescence study of uranyl coordination polymers containing chelating terpyridine and trispyridyltriazine ligands. *CrystEngComm* **2015**, *17*, 6236−6247. (b) Thangavelu, S. G.; Cahill, C. L. A Family of Uranyl Coordination Polymers Containing O-Donor Dicarboxylates and Trispyridyltriazine Guests. *Cryst. Growth Des.* **2016**, *16* (1), 42−50.

(14) Thuéry, P. 2,2′ Bipyridine and 1,10 Phenanthroline as Coligands or Structure Directing Agents in Uranyl−Organic Assemblies with Polycarboxylic Acids. *Eur. J. Inorg. Chem.* **2013**, *2013*, 4563−4573.

(15) *SAINT*; Bruker AXS Inc.: Madison, WI, 2007.

(16) *APEX III*; Bruker AXS Inc.: Madison, WI, 2016.

(17) Krause, L.; Herbst-Irmer, R.; Sheldrick, G. M.; Stalke, D. Comparison of silver and molybdenum microfocus X-ray sources for single-crystal structure determination. *J. Appl. Crystallogr.* **2015**, *48*, 3−10.



DOI: 10.1021/acs.inorgchem.9b00255
*Inorg. Chem.* 2019, 58, 7243−7254

(18) Sheldrick, G. M. Crystal structure refinement with SHELXL. *Acta Crystallogr., Sect. A: Found. Adv.* **2015**, *A71*, 3−8.
(19) Farrugia, L. J. WinGX and ORTEP for Windows: an update. *J. Appl. Crystallogr.* **2012**, *45*, 849−854.
(20) Spek, A. L. Structure validation in chemical crystallography. *Acta Crystallogr., Sect. D: Biol. Crystallogr.* **2009**, *65*, 148−155.
(21) *Crystal Maker*; Crystal Maker Software Limited: Bicester, England, 2009.
(22) Putz, H.; Brandenburg, K. *Match! − Phase Identification from Powder Diffraction*; Crystal Impact: Bonn, Germany, 2015.
(23) Farago, M. E.; Amirhaeri, S. Malonates of bi- and ter-valent metal ions. *Inorg. Chim. Acta* **1984**, *81*, 205−212.
(24) Cheetham, A. K.; Rao, C. N. R.; Feller, R. K. Structural diversity and chemical trends in hybrid inorganic−organic framework materials. *Chem. Commun.* **2006**, 4780−4795.
(25) Li, P.; Vermeulen, N. A.; Gong, X.; Malliakas, C. D.; Stoddart, J. F.; Hupp, J. T.; Farha, O. K. Design and Synthesis of a Water-Stable Anionic Uranium-Based Metal−Organic Framework (MOF) with Ultra Large Pores. *Angew. Chem., Int. Ed.* **2016**, *55*, 10358−10362.
(26) (a) Li, P.; Vermeulen, N. A.; Gong, X.; Malliakas, C. D.; Stoddart, J. F.; Hupp, J. T.; Farha, O. K. Design and Synthesis of a Water-Stable Anionic Uranium-Based Metal-Organic Framework (MOF) with Ultra Large Pores. *Angew. Chem.* **2016**, *128*, 10514−10518. (b) Cavka, J. H.; Jakobsen, S.; Olsbye, U.; Guillou, N.; Lamberti, C.; Bordiga, S.; Lillerud, K. P. *J. Am. Chem. Soc.* **2008**, *130*, 13850−13851. (c) Park, K. S.; Ni, Z.; Côté, A. P.; Choi, J. Y.; Huang, R.; Uribe-Romo, F. J.; Chae, H. K.; O'Keeffe, M.; Yaghi, O. M. *Proc. Natl. Acad. Sci. U. S. A.* **2006**, *103*, 10186.
(27) (a) Alexandrov, E. V.; Blatov, V. A.; Kochetkov, A. V.; Proserpio, D. M. Underlying nets in three-periodic coordination polymers: topology, taxonomy and prediction from a computer-aided analysis of the Cambridge Structural Database. *CrystEngComm* **2011**, *13*, 3947−3958. (b) O'Keeffe, M.; Yaghi, O. M. Deconstructing the Crystal Structures of Metal-Organic Frameworks and Related Materials into Their Underlying Nets. *Chem. Rev.* **2012**, *112*, 675−702.
(28) O'Keeffe, M.; Peskov, M. A.; Ramsden, S. J.; Yaghi, O. M. The Reticular Chemistry Structure Resource (RCSR) database of, and symbols for, crystal nets. *Acc. Chem. Res.* **2008**, *41*, 1782−1789. RCSR can be accessed at http://rcsr.anu.edu.au.
(29) (a) Blatov, V. A. *IUCr Computing Commission Newsletter*; IUCr: Chester, U.K., 2006; No. 7, pp 4−38. (b) Blatov, V. A.; Shevchenko, A. P.; Proserpio, D. M. Applied Topological Analysis of Crystal Structures with the Program Package ToposPro. *Cryst. Growth Des.* **2014**, *14*, 3576−3586.
(30) Yang, Z.; Chen, N.; Wang, C.; Yan, L.; Li, G. Syntheses, Crystal Structures, and Properties of Four Complexes Constructed From 2-Propyl-1H-Imidazole-4,5- Dicarboxylic Acid. *Synth. React. Inorg., Met.-Org., Nano-Met. Chem.* **2012**, *42* (3), 336−344.
(31) Cahill, C. L.; de Lill, D. T.; Frisch, M. Homo- and heterometallic coordination polymers from the f elements. *CrystEngComm* **2007**, *9*, 15−26.
(32) Li, P.; Vermeulen, N. A.; Malliakas, C. D.; Gómez-Gualdrón, D. A.; Howarth, A. J.; Mehdi, B. L.; Dohnalkova, A.; Browning, N. D.; O'Keeffe, M.; Farha, O. K. Bottom-up construction of a superstructure in a porous uranium-organic crystal. *Science* **2017**, *356*, 624−627.
(33) Zhao, R.; Mei, L.; Hu, K.-Q.; Wang, L.; Chai, Z.-F.; Shi, W.-Q. Two Three Dimensional Actinide Silver Heterometallic Coordination Polymers Based on 2,2′ Bipyridine 3,3′ dicarboxylic Acid with Helical Chains Containing Dimeric or Trimeric Motifs. *Eur. J. Inorg. Chem.* **2017**, *2017*, 1472−1477.
(34) Zhao, R.; Mei, L.; Hu, K. Q.; Tian, M.; Chai, Z. F.; Shi, W. Q. Bimetallic Uranyl Organic Frameworks Supported by Transition-Metal-Ion-Based Metalloligand Motifs: Synthesis, Structure Diversity, and Luminescence Properties. *Inorg. Chem.* **2018**, *57* (10), 6084−6094.
(35) Thuéry, P.; Masci, B. Uranyl−organic one- and two-dimensional assemblies with 2,2′-bipyridine-3,3′-dicarboxylic, biphenyl-3,3′,4,4′-tetracarboxylic and bicyclo[2.2.2]oct-7-ene-2,3,5,6-tetracarboxylic acids. *CrystEngComm* **2012**, *14*, 131−137.
(36) (a) Knope, K. E.; Soderholm, L. Solution and Solid-State Structural Chemistry of Actinide Hydrates and Their Hydrolysis and Condensation Products. *Chem. Rev.* **2013**, *113*, 944−994. (b) Baes, C. F.; Mesmer, R. E. *The Hydrolysis of Cations*; John Wiley and Sons: New York, NY, 1976.
(37) Grenthe, I.; Fuger, J.; Konings, R. J. M.; Lemire, R. J.; Nguyen-Trun, C.; Wanner, H. *Chemical Thermodynamics of Uranium*; Organization for Economic Cooperation and Development: Issy-les Moulineaux, France, 2004.
(38) Spek, A. L. PLATON, An Integrated Tool for the Analysis of the Results of a Single Crystal Structure Determination. *Acta Crystallogr., Sect. A* **1990**, *46*, C-34.
(39) Denning, R. G. Electronic structure and bonding in actinyl ions and their analogs. *J. Phys. Chem. A* **2007**, *111*, 4125−4143.
(40) Thuéry, P.; Harrowfield, J. Uranyl−Organic Frameworks with Polycarboxylates: Unusual Effects of a Coordinating Solvent. *Cryst. Growth Des.* **2014**, *14*, 1314−1323.
(41) (a) Chen, W.; Wang, J.-Y.; Chen, C.; Yue, Q.; Yuan, H.-M.; Chen, J.-S.; Wang, S.-N. Photoluminescent metal-organic polymer constructed from trimetallic clusters and mixed carboxylates. *Inorg. Chem.* **2003**, *42* (4), 944−946. (b) Tsushima, S. On the "yl" bond weakening in uranyl(VI) coordination complexes. *Dalton Trans.* **2011**, *40*, 6732−6737.
(42) (a) Redmond, M. P.; Cornet, S. M.; Woodall, S. D.; Whittaker, D.; Collison, D.; Helliwell, M.; Natrajan, L. S. Probing the local coordination environment and nuclearity of uranyl(VI) complexes in non-aqueous media by emission spectroscopy. *Dalton Trans.* **2011**, *40*, 3914−3926. (b) Carter, K. P.; Kalaj, M.; Cahill, C. L. Probing the Influence of N Donor Capping Ligands on Supramolecular Assembly in Molecular Uranyl Materials. *Eur. J. Inorg. Chem.* **2016**, *2016*, 126−137.
(43) (a) Boutinaud, P.; Putaj, P.; Mahiou, R.; Cavalli, E.; Speghini, A.; Bettinelli, M. Quenching of Lanthanide Emission by Intervalence Charge Transfer in Crystals Containing Closed Shell Transition Metal Ions. *Spectrosc. Lett.* **2007**, *40*, 209−220. (b) Blasse, G. Optical electron transfer between metal ions and its consequences. In *Complex Chemistry*; Structure and Bonding; Springer: Berlin,1991; Vol. 76. (c) Burrows, H. D.; Formosinho, S. J.; Da Graca Miguel, M.; Coelho, F. P. Quenching of the luminescent state of the uranyl ion ($UO_2^{+2}$) by metal ions. Evidence for an electron transfer mechanism. *J. Chem. Soc., Faraday Trans. 1* **1976**, *72*, 163−171. (d) Frisch, M.; Cahill, C. L. Syntheses, structures and fluorescent properties of two novel coordination polymers in the U−Cu−H 3 pdc system. *Dalton Trans.* **2005**, 1518−1523. (e) Thuery, P.; Riviere, E.; Harrowfield, J. Uranyl and uranyl-3d block cation complexes with 1,3-adamantanedicarboxylate: crystal structures, luminescence, and magnetic properties. *Inorg. Chem.* **2015**, *54*, 2838−2850.
(44) Tits, J.; Walther, C.; Stumpf, T.; Macé, N.; Wieland, E. A luminescence line-narrowing spectroscopic study of the uranium(VI) interaction with cementitious materials and titanium dioxide. *Dalton Trans.* **2015**, *44*, 966−976.
(45) Bünzli, J. C.G.; Eliseeva, S. V. Basics of Lanthanide Photophysics. In *Lanthanide Luminescence*; Hänninen, P., Härmä, H., Eds.; Springer Series on Fluorescence (Methods and Applications); Springer: Berlin, 2010; Vol. 7.
(46) Liu, Q.; Zhang, Q.; Yang, S.; Zhu, H.; Liu, Q.; Tian, G. Raman spectral titration method: an informative technique for studying the complexation of uranyl with uranyl(VI)−DPA/oxalate systems as examples. *Dalton Trans.* **2017**, *46*, 13180−13187.


DOI: 10.1021/acs.inorgchem.9b00255
*Inorg. Chem.* 2019, 58, 7243−7254